Chapter

Study on Dislocation-Dopant Ions Interaction during Plastic Deformation by Combination Method of Strain-Rate Cycling Tests and Application of Ultrasonic Oscillations

Yohichi Kohzuki

Abstract

Strain-rate cycling tests associated with the ultrasonic oscillation were conducted for the purpose of investigation on the interaction between dislocation and dopant ions during plastic deformation of seven kinds of single crystals: NaCl doped with Li^+, K^+, Rb^+, Cs^+, F^-, Br^- or I^- ions separately. Relative curves between the stress decrement ($\Delta\tau$) due to ultrasonic oscillatory stress and strain-rate sensitivity (λ) of flow stress under superposition of the oscillation are obtained by the original method (combination method of strain-rate cycling tests and application of ultrasonic oscillations) at 77 K to room temperature and have stair-like shapes for the specimens at low temperatures. The Gibbs free energy for overcoming of the dopant ion by dislocation at absolute zero is calculated from the data analyzed in terms of $\Delta\tau$ vs. λ. As a result, the obtained energies are found to be varied linearly with the isotropic defect around it in the each specimen.

Keywords: dislocation, ultrasonic oscillatory stress, activation energy, monovalent ion, isotropic strain

1. Introduction

Dislocation (linear defects in crystal) motions are related to the plasticity of crystal in a microscopic viewpoint. It is well known that the solution hardening depends on dislocation motion hindered by the atomic defects around impurities in crystals and is namely influenced by the dislocation-point defects interaction, which has been widely investigated by various methods. For instance, measurements of yield stress (e.g., [1–7]) and proof stress (e.g., [8, 9]), micro-hardness tests (e.g., [10–14]), direct observations of dislocation (e.g., [15–21]), internal friction measurements (e.g., [22–27]), or stress relaxation tests (e.g., [28, 29]) have been carried out so far. Nevertheless, it is difficult to obtain such information on the motion of the dislocation which moves by overcoming the forest dislocations and the weak obstacles such as impurities during plastic deformation of bulk. A large

number of investigations have been conducted by the separation of the flow stress into effective and internal stresses on the basis of the temperature dependence of yield stress, the strain rate dependence of flow stress, and the stress relaxation. Yield stress depends on dislocation velocity, dislocation density, and multiplication of dislocations [30]. On the other hand, the effect of heat treatment on the microhardness is almost insensitive to the change of atomic order of point defects in a specimen. As for direct observations, electron microscopy provides the information on dislocation motion for a thin specimen but not for bulk, and also light scattering method is useful only for a transparent specimen. X-ray topography is the lack of resolution in the photograph, so that the specimen is limited to the low dislocation density below 10^4 cm^{-2}. Internal friction measurements concern the motion of the dislocation which breaks away from the weak obstacles between two forest dislocations by vibration [31]. Stress relaxation tests are generally assumed that internal structure of crystals does not change, i.e., dislocation density and internal stress are constant. Above-mentioned methods cannot provide the information on dislocation-obstacles interaction in bulk during plastic deformation.

In this chapter, the study on interaction between a dislocation and dopant ions is made by the strain-rate cycling tests during the Blaha effect measurement. The original method (strain-rate cycling tests associated with the Blaha effect measurement) is different from above-mentioned ones and would be possible to clear up it. The Blaha effect is the phenomenon that static flow stress decreases when an ultrasonic oscillatory stress is superimposed during plastic deformation [32]. Ohgaku and Takeuchi [33, 34] reported that the strain-rate cycling under the application of oscillation can separate the contributions arising from the interaction between a dislocation and dopant ions and from the dislocations themselves during plastic deformation at room temperature. Using ionic single crystals of KCl doped with Br^- (0.5, 1.0, and 2.0 mol%) or I^- (0.2, 0.5, and 1.0 mol%) [35] and of NaCl doped with Br^- (0.1, 0.5, and 1.0 mol%) [36], they discussed temperature dependence of the effective stress due to monovalent dopants (i.e., Br^- or I^-) and found that the measurement of strain-rate sensitivity under the ultrasonic oscillatory stress provides useful information on a mobile dislocation-the dopant ions interaction [35, 36]. The information on the dislocation motion breaking-away from dopant ions [37–40] and also X-irradiation induced defects [41] with the ultrasonic oscillatory stress has been successively provided by the original method, which seemed to separate the contributions arising from the dislocation-the point defects interaction and from dislocations themselves during plastic deformation of crystals.

The Blaha effect was found by Blaha and Langenecker when the ultrasonic oscillatory stress of 800 kHz was superimposed during plastic deformation of Zn single crystals. The same phenomenon as Zn crystals has been also observed in many metals (e.g., [42–44]). Since this phenomenon has a significance as an industrial purpose, it has been widely made to apply to the plastic working technique: wire drawing, deep drawing, rolling, and another metal forming techniques (e.g., [45–53]).

The strain-rate cycling tests associated with ultrasonic oscillation were carried out here for NaCl single crystals doped with various monovalent ions separately. The monovalent ion is considered to have isotropic strain in the alkali halide crystal because its size is different from the substituted ion of the host crystal. Dopant ions are expected to cause the hardening due to the dislocation motion hindered by the defects around them at low temperature. Its force-distance profile between a dislocation and an atomic defect is expressed by Cottrell and Bilby [54]. This chapter refers to the energy supplied by the thermal fluctuations, when the dopant ions are overcome by a dislocation with the help of thermal activation during plastic deformation of crystals. This is estimated from the dependence of the effective stress

due to impurities on activation volume, which reveals the force-distance profile, given by the measurement of the stress decrement due to application of ultrasonic oscillatory stress and strain-rate sensitivity of flow stress under superimposition of ultrasonic oscillation. And further, it is presented that the difference in size of isotropic strain around the various dopants different from host ion has an influential factor of the energy for overcoming the dopant ion by a dislocation in several kinds of alkali-halide single crystals.

2. Combination method of strain-rate cycling tests and the Blaha effect measurement

Specimens used in this work were seven kinds of single crystals: NaCl doped with Li^+, K^+, Rb^+, Cs^+, F^-, Br^- or I^- ions separately. Each concentration of the dopants was 0.5 mol% in the melt. The specimens were prepared by cleaving the single crystalline ingots, which were grown by the Kyropoulos method [55] in air, to the size of 5 × 5 × 15 mm^3. Furthermore, they were kept immediately below the melting point for 24 h and were gradually cooled to room temperature at a rate of 40 K h^{-1}. This heat treatment was carried out for the purpose of reducing dislocation density as much as possible.

The schematic illustration of apparatus is shown in **Figure 1**. A resonator composed of a vibrator and a horn was attached to the testing machine, INSTRON Type 4465. The specimens were lightly fixed on a piezoelectric transducer and then cooled down to a test temperature. Each specimen was held at the test temperature for 30 min prior to the following test. The specimens were deformed by compression along the <100> axis at 77 K up to the room temperature, and the ultrasonic oscillatory stress was intermittently superimposed for 1 or 2 min by the resonator in the same direction as the compression. The temperature measurements of specimens were conducted by heater controlled using thermocouples of Ni-55%Cu vs. Cu. As for the tests at 77 K, the specimen was immersed in the liquid nitrogen. The stability of temperature during the test was kept within 2 K. The resonant frequency was 20 kHz from a multifunction synthesizer and the amplitude of the oscillatory

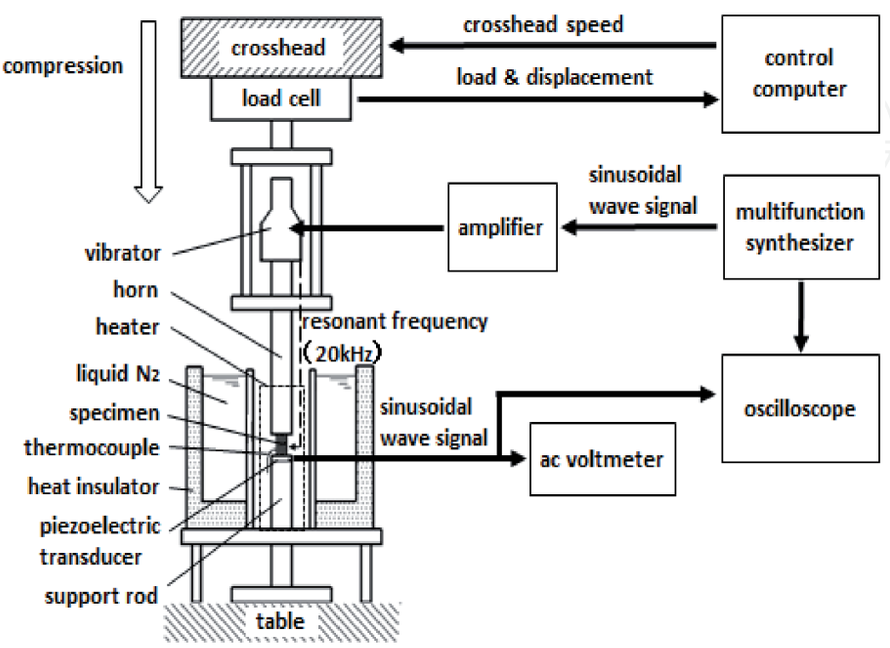

Figure 1.
Schematic block diagram of apparatus system.

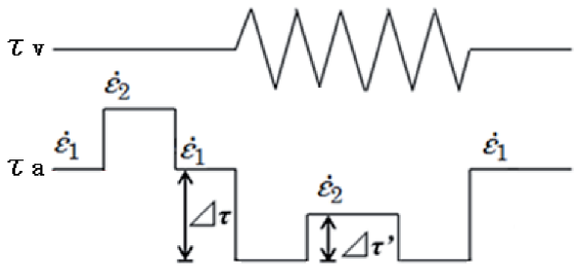

Figure 2.
Explanatory diagram of a change in applied shear stress, τ_a, for the strain-rate cycling test between the strain rates, $\dot{\varepsilon}_1$ ($2.2 \times 10^{-5}\ s^{-1}$) and $\dot{\varepsilon}_2$ ($1.1 \times 10^{-4}\ s^{-1}$), under superposition of ultrasonic oscillatory shear stress, τ_v.

stress was monitored by the output voltage from the piezoelectric transducer set between a specimen and the support rod, which was observed by an a.c. voltmeter or an oscilloscope. Since the wavelength, which is 226 mm on the basis of calculating from the data of ref. [56], is 15 times as long as the length of specimen, the strain of specimen is supposed to be homogeneous.

Strain-rate cycling tests made between the crosshead speeds of 10 and 50 μm min^{-1} were performed within the temperatures. The strain-rate cycling test associated with the ultrasonic oscillation is illustrated in **Figure 2**. Superposition of oscillatory stress (τ_v) causes a stress drop ($\Delta\tau$) during plastic deformation. When the strain-rate cycling between strain-rates of $\dot{\varepsilon}_1$ ($2.2 \times 10^{-5}\ s^{-1}$) and $\dot{\varepsilon}_2$ ($1.1 \times 10^{-4}\ s^{-1}$) was carried out keeping the stress amplitude of τ_v constant, the variation of stress due to the strain-rate cycling is $\Delta\tau$'. The strain-rate sensitivity ($\Delta\tau'/\Delta\ln\dot{\varepsilon}$) of the flow stress, which is given by $\Delta\tau'/1.609$, was used as a measurement of the strain-rate sensitivity ($\lambda = \Delta\tau'/\Delta\ln\dot{\varepsilon}$). Slip system for rock-salt structure such as NaCl crystal is {110} <1$\bar{1}$0> so that shear stress (τ) and shear strain (ε) calculated for the slip system were used in this study.

3. Relation between stress decrement ($\Delta\tau$) and strain-rate sensitivity (λ)

Figure 3 shows the influence of temperature on $\Delta\tau$ vs. λ curve for the NaCl:Rb^+ (0.5 mol%) single crystals at strain 6%. The variation of λ with $\Delta\tau$ has stair-like shape: two bending points and two plateau regions are on the each curve. That is to say, the first plateau region ranges below the first bending point at low $\Delta\tau$ and the second one extends from the second bending point at high $\Delta\tau$. λ gradually decreases with increasing $\Delta\tau$ between the two bending points. The length of $\Delta\tau$ within the first plateau region is named τ_p as denoted in **Figure 3**. τ_p tends to be lower at higher temperature. Similar phenomena as **Figure 3** are observed for all the other NaCl single crystals contained with the monovalent impurities (i.e. Li^+, K^+, Cs^+, F^-, Br^- or I^- ions).

The relation between $\Delta\tau$ and λ reflects the effect of ultrasonic oscillation on the dislocation motion on the slip plane containing many weak obstacles such as impurities and a few forest dislocations during plastic deformation [40]. $\Delta\tau$ vs. λ curve is divided into three regions as shown in **Figure 3**. Within the first plateau region of relative curve (i.e. region 1 in **Figure 3**), the application of oscillation with low stress amplitude cannot influence the average length of dislocation segments ($\bar{l}$) and $\bar{l}$ is considered to remain constant. All weak obstacles act as impedimenta to the dislocation motion there. In region 2, the dislocation begins to break-away from the weak ones between the forest dislocations by applying oscillation with high stress amplitude. As a result, $\bar{l}$ begins to increase and the λ of flow stress starts to decrease at the stress decrement $\Delta\tau$ of τ_p. This is because λ is inversely proportional to $\bar{l}$ [57].

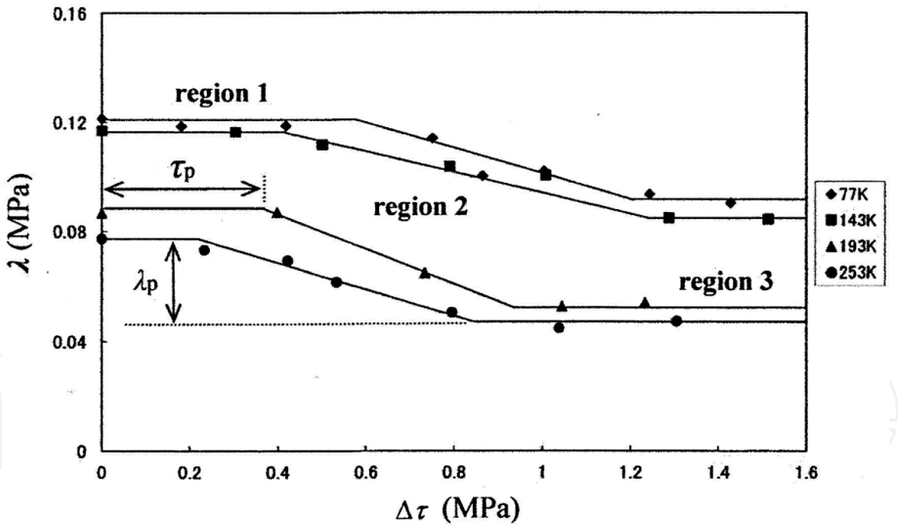

Figure 3.
Relation between the stress decrement ($\Delta\tau$) and the strain-rate sensitivity (λ) for NaCl:Rb^+ (0.5 mol%) at strain 6% and various temperatures. The numbers besides each symbol represent the temperature (reproduced from Ref. [58] with permission from the publisher).

Some weak obstacles stop acting as impedimenta in the region. The weak obstacles are supposed to be monovalent dopants (Li^+, K^+, Rb^+, Cs^+, F^-, Br^- or I^- ions) and not to be vacancies here, since the vacancies have low density as against the dopants in the specimen. When the specimens were plastically deformed, it is imagined that a dislocation begins to overcome from the dopants which lie on the dislocation with the help of thermal activation. Then, τ_p is considered to represent the effective stress due to the ions. Accordingly, τ_p is expected to decrease with increasing temperature. $\Delta\tau$ vs. λ curves shown in **Figure 3** correspond to this. As the temperature becomes larger, τ_p shifts in the direction of lower $\Delta\tau$. τ_p depends on type and density of the weak obstacle [36, 38]. Applying still larger stress amplitude during plastic deformation of the specimens, the second plateau region within stage 3 becomes to appear on the relative curves in **Figure 3**. In stage 3, the dopants are no longer act as the impedimenta to mobile dislocations and the dislocations are hindered only by forest dislocations. Then, $\bar{l}$ becomes constant again. This leads to the constant λ of flow stress. λ_p denoted in **Figure 3** is introduced later.

4. Model overcoming the thermal obstacle by a dislocation

A dislocation will encounter a stress field illustrated schematically in **Figure 4** as it moves through on the slip plane containing many weak obstacles and a few strong ones. In the figure, the positive stress concerning axis of the ordinate opposes the flow stress (applied stress τ) and the negative stress assists it. Extrinsic resistance to the dislocation motion has two types: one is long-range obstacle (the order of 10 atomic diameters or greater) and the other short-range obstacle (less than about 10 atomic diameters). The former is considered to be forest dislocations, large precipitates or second-phase particles, and grain boundary, for instance, and the latter impurity atoms, isolated and clustered point defects, small precipitates, intersecting dislocations, etc. Overcoming the latter type of obstacles (byname, thermal obstacles) by a dislocation, thermal fluctuations play an important role in aid of the flow stress above the temperature of 0 K. Then the aid energy, ΔG, supplied by the thermal fluctuations is given by the shaded part in **Figure 4**. Thus the dislocation can move through below τ_0 (i.e. effective stress τ^* due to short-range obstacles and internal stress τ_i

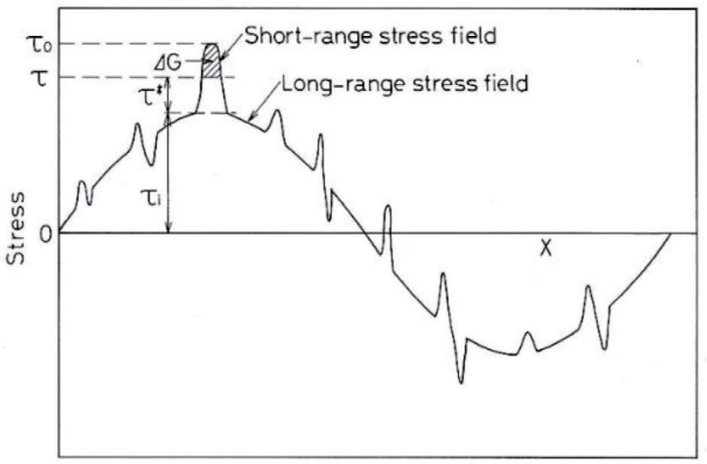

Figure 4.
Stress fields encountered by a dislocation moving through the crystal lattice [57].

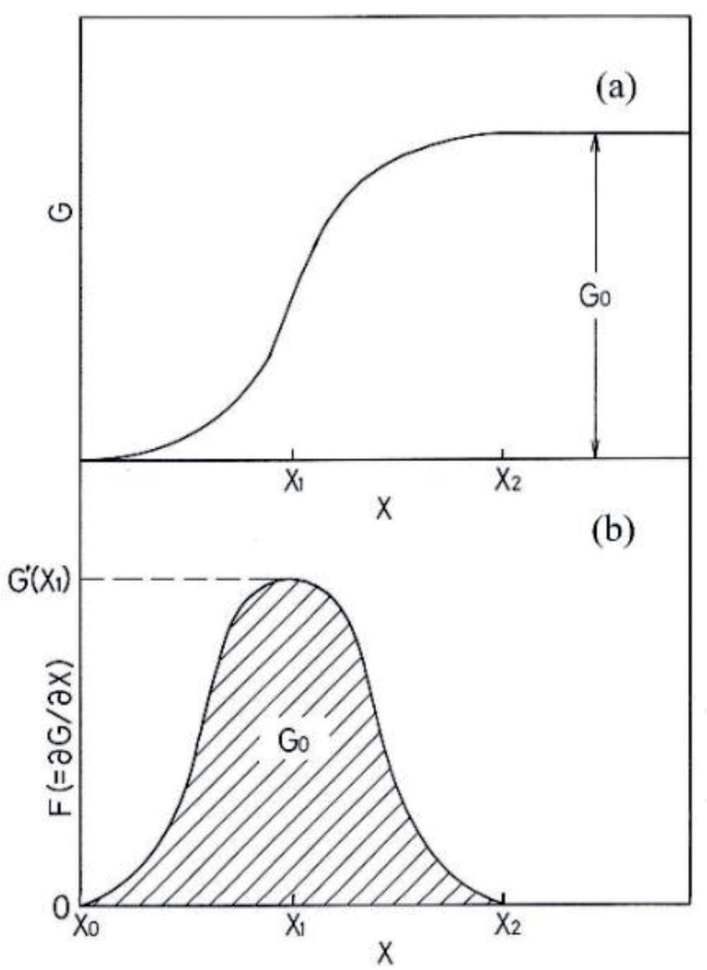

Figure 5.
The process for thermal activated overcoming of the short-range obstacle by a dislocation. Variation in (a) the Gibbs free energy of activation and (b) the force acted on the dislocation with the distance for a dislocation motion [57].

due to long-range ones in **Figure 4**). τ_0 is the value of τ at 0 K. As for the long-range obstacles (byname, athermal obstacles), the energy barrier is so large that the thermal fluctuations play no role in overcoming them within the temperature range.

The representation of **Figure 5** is concerned with a common type of thermal activation barrier. The free energy (G) varies with the distance (x) between a

dislocation and the obstacle as given in **Figure 5(a)**. When a dislocation overcomes the short-range obstacles, the free energy becomes high on account of the work (ΔW) done by the applied stress. Then the resistance (F), where it can be defined by the differentiation of free energy with respect to x (i.e. $\partial G/\partial x$), to the dislocation motion is revealed as **Figure 5(b)** in accord with the abscissa of **Figure 5(a)**. F value is maximum at position x_1. **Figure 5(b)** corresponds to typical force-distance curve for short-range obstacle among those in **Figure 4**. Shape of this curve represented by $F(x)$ means the model overcoming the obstacle by a dislocation. G_0, which is taken as the shaded area under $F(x)$ between saddle-point positions x_0 and x_2 in **Figure 5(b)**, is the Gibbs free energy of activation for the breakaway of the dislocation from the obstacle in the absence of an applied stress (in this case it is equivalent to the Helmholtz free energy for the dislocation motion).

5. Relation between the effective stress due to impurities on activation volume

When the dislocation breaks-away from the defects on a slip plane with the aid of thermal activation during plastic deformation, observations of τ_p and λ_p would provide information on the dislocation-defect interaction in the specimen. λ_p is the difference between λ at first plateau place and at second one on $\Delta\tau$ vs. λ curve as presented in **Figure 3**, which has been regarded as the component of strain-rate sensitivity due to dopant ions when a dislocation moves forward with the help of oscillation [40].

Figure 6 shows the relation between τ_p and activation volume (V) for NaCl:Rb^+ (0.5 mol%). The activation volume has been expressed as [57].

$$V = kT\left(\frac{\partial \ln \dot{\varepsilon}}{\partial \tau}\right) \tag{1}$$

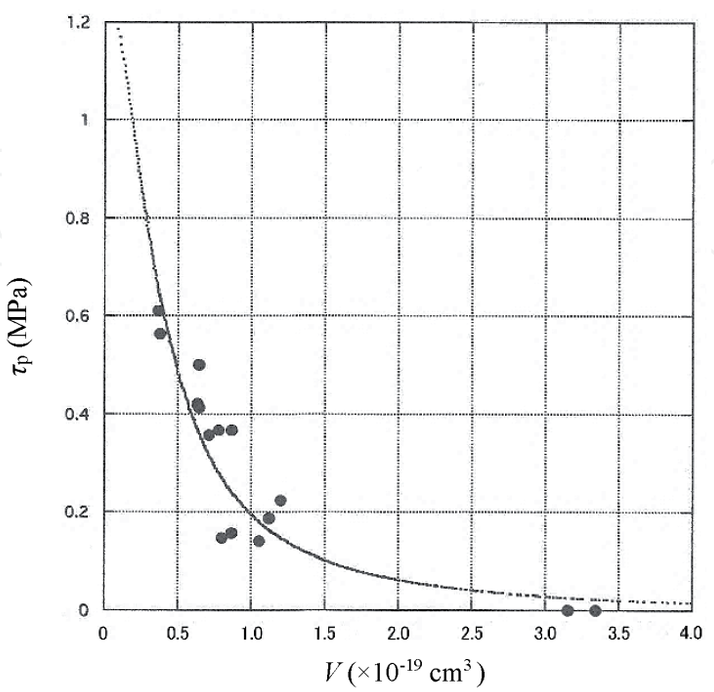

Figure 6.
Relation between τ_p and activation volume (V) for NaCl:Rb^+ (0.5 mol%) (reproduced from Ref. [58] with permission from the publisher).

Specimen	G_0 (eV)
NaCl:Li^+ (0.5 mol%)	0.55
NaCl:K^+ (0.5 mol%)	0.60
NaCl:Rb^+ (0.5 mol%)	0.61
NaCl:Cs^+ (0.5 mol%)	0.82
NaCl:F^- (0.5 mol%)	0.69
NaCl:Br^- (0.5 mol%)	0.47
NaCl:I^- (0.5 mol%)	0.53

Table 1.
Values of energy G_o.

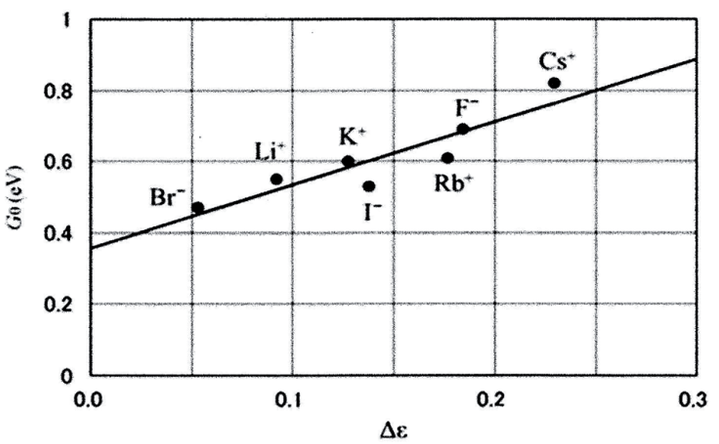

Figure 7.
Variation of the interaction energy (G_o) *between dislocation and the dopant ion with the defect size (reproduced from Ref. [58] with permission from the publisher).*

where k is the Boltzmann constant and T is the absolute temperature. Here, the $\left(\frac{\partial \ln \dot{\varepsilon}}{\partial \tau}\right)$ in Eq. (1) is obtained from λ_p. Eq. (1) is namely replaced by

$$V = kT/\lambda_p. \tag{2}$$

This dependence (τ_p vs. V) also represents the force-distance profile between dislocation and Rb^+ ion. The τ_p vs. V curve gives the value of G_0 for the specimen. The G_0 values for the other specimens (i.e. NaCl: Li^+, K^+, Cs^+, F^-, Br^- or I^-) are similarly estimated and are listed in **Table 1**.

Figure 7 shows the obtained energies G_0 with the isotropic defect size ($\Delta\varepsilon$), which is estimated from the difference between the lattice constants of host crystal and dopant, around ion doped in the each specimen. The ions beside each plot represent the dopants in NaCl single crystals. G_0 values vary linearly with $\Delta\varepsilon$ in the specimens. The intercept of the straight line is 0.36 eV, which is considered to be the interaction energy between dislocation and inherent obstacle of the host crystal because $\Delta\varepsilon$ is zero.

6. Conclusions

The following conclusions were derived from the data analyzed in terms of the $\Delta\tau$ vs. λ curves for NaCl: Li^+, K^+, Rb^+, Cs^+, Br^-, I^-, F^-, Br^- or I^- single crystals.

1. The relation between $\Delta\tau$ and λ has stair-like shape for the specimens at a given temperature and strain. There are two bending points and two plateau regions. λ decreases with $\Delta\tau$ between the two bending points. The measurement of τ_p and V calculated with λ_p provides information on the interaction between mobile dislocation and the dopant ion in the specimens during plastic deformation.

2. The Gibbs free energy G_0 for the overcoming of dislocation from the dopant is obtained for each of the specimens and increases linearly with increasing the defect size $\Delta\varepsilon$. This result leads to the conclusion that the dopant ion as weak obstacle to dislocation motion becomes slightly stronger with larger defect size around the dopant in NaCl single crystal.

Acknowledgements

Dr. T. Ohgaku, as well as S. Yamaguchi, M. Azuma, H. Teraji, E. Ogawa and Y. Yamanaka are acknowledged for his collaboration in the analysis on $\Delta\tau$ and λ data, as well as for their experimental assistance.

Conflict of interest

The author declares no conflict of interest.

Author details

Yohichi Kohzuki
Department of Mechanical Engineering, Saitama Institute of Technology, Fukaya, Japan

*Address all correspondence to: kohzuki@sit.ac.jp

References

[1] Chin GY, Van Uitert LG, Green ML, Zydzik GJ, Kometani TY. Strengthening of alkali halides by divalent-ion additions. Journal of the American Ceramic Society. 1973;**56**:369-372. DOI: 10.1111/j.1151-2916.1973.tb12688.x

[2] Suszyńska M. Effect of impurity concentration and plastic deformation on dislocation density of KCl crystals. Kristall und Technik. 1974;**9**:1199-1207. DOI: 10.1002/crat.19740091015

[3] Kataoka T, Yamada T. Yield strength and dislocation mobility of KCl-KBr solid solution single crystals. Japanese Journal of Applied Physics. 1977;**16**:1119-1126. DOI: 10.1143/JJAP.16.1119

[4] Boyarskaya YS, Zhitaru RP, Palistrant NA. The anomalous behaviour of the doped NaCl crystals compressed at low temperatures. Crystal Research and Technology. 1990;**25**:1469-1473. DOI: 10.1002/crat.2170251219

[5] Boyarskaya YS, Zhitaru RP, Palistrant NA. Influence of the state of the impurity on the deformation-rate dependence of the yield stress of NaCl:Ca single crystals. Soviet Physics - Solid State. 1990;**32**:1989-1990

[6] Okazaki K. Solid-solution hardening and softening in binary iron alloys. Journal of Materials Science. 1996;**31**:1087-1099. DOI: 10.1007/BF00352911

[7] Tabachnikova ED, Podolskiy AV, Smirnov SN, Psaruk IA, Liao PK. Temperature dependent mechanical properties and thermal activation plasticity of nanocrystalline and coarse grained Ni-18.75 at.% Fe alloy. IOP Conference Series: Materials Science and Engineering. 2014;**63**:012105. DOI: 10.1088/1757-899X/63/1/012105

[8] Pratt PL, Harrison RP, Newey CWA. Dislocation mobility in ionic crystals. Discussions of the Faraday Society. 1964;**38**:211-217. DOI: 10.1039/DF9643800211

[9] Newey CWA, Harrison RP, Pratt PL. Precipitation hardening and dislocation locking in doped NaCl. Proceedings of the British Ceramic Society. 1966;**6**:305-316

[10] Chin GY, Van Uitert LG, Green ML, Zydzik G. Hardness, yield strength and Young's modulus in halide crystals. Scripta Metallurgica. 1972;**6**:475-480. DOI: 10.1016/0036-9748(72)90031-2

[11] Green ML, Zydzik G. Effect of heat treatment on the microhardness of some mixed and doped alkali halides. Scripta Metallurgica. 1972;**6**:991-994. DOI: 10.1016/0036-9748(72)90159-7

[12] Andreev GA, Klimov VA. Influence of the state of an impurity on the microhardness of NaCl:Sr single crystals. Soviet Physics - Solid State. 1980;**22**:2042-2043

[13] Buravleva MG, Rozenberg GK, Soifer LM, Chaikovskii EF. Changes in the flow stress of LiF:Mg^{2+} and LiF:Co^{2+} crystals during precipitation of solid solutions. Soviet Physics - Solid State. 1980;**22**:150-152

[14] Narasimha Reddy K, Subba Rao UV. Influence of gadolonium impurity on microhardness of host alkali halide crystal. Crystal Research and Technology. 1984;**19**:K73-K76. DOI: 10.1002/crat.2170190730

[15] Strunk H. Investigation of cross-slip events in NaCl crystals by transmission electron microscopy. Physica Status Solidi (A). 1975;**28**:119-126. DOI: 10.1002/pssa.2210280111

[16] Appel F, Messerschmidt U. The interaction between dislocations and point obstacles: A comparison of the

interaction parameter distributions obtained from computer simulation and from in situ high voltage electron microscopy straining experiments. Materials Science and Engineering: A. 1982;**52**:69-74. DOI: 10.1016/0025-5416(82)90070-2

[17] Messerschmidt U, Appel F, Schmid H. The radius of curvature of dislocation segments in MgO crystals stressed in the high-voltage electron microscope. Philosophical Magazine A. 1985;**51**:781-796. DOI: 10.1080/01418618508237587

[18] Kataoka T, Ohji H, Morishita H, Kishida K, Azuma K, Yamada T. In-situ observation of moving dislocations in KCl crystal by laser-light topography. Japanese Journal of Applied Physics. 1989;**28**:L697-L700. DOI: 10.1143/JJAP.28.L697

[19] Kataoka T, Ohji H, Kishida K, Azuma K, Yamada T. Direct observation of glide dislocations in a KCl crystal by the light scattering method. Applied Physics Letters. 1990;**56**:1317-1319. DOI: 10.1063/1.102504

[20] Kataoka T. The light scattering topography method: Direct observation of moving dislocations. Butsuri. 1992;**47**:713-716. (in Japanese)

[21] Messerschmidt U. Dislocation Dynamics during Plastic Deformation. Berlin Heidelberg: Springer; 2010. DOI: 10.1007/978-3-642-03177-9

[22] Indenbom VL, Chernov VM. Determination of characteristics for the interaction between point defects and dislocations from internal friction experiments. Physica Status Solidi A: Applications and Material Science. 1972;**14**:347-354. DOI: 10.1002/pssa.2210140142

[23] Schwarz RB, Granato AV. Measurement of the force-distance profile for the interaction between a dislocation and a point defect. Physical Review Letters. 1975;**34**:1174-1177. DOI: 10.1103/PhysRevLett.34.1174

[24] Ivanov VI, Lebedev AB, Kardashev BK, Nikanorov SP. Interaction of dislocations with pinning centers in magnesium at temperatures 295-4.2K. Soviet Physics - Solid State. 1986;**28**:867-868

[25] Kosugi T, Kino T. Experimental determination of the force-distance relation for the interaction between a dislocation and a solute atom. Journal of the Physical Society of Japan. 1987;**56**:999-1009. DOI: 10.1143/JPSJ.56.999

[26] Kosugi T. Temperature dependence of amplitude-dependent internal friction due to simultaneous breakaway of a dislocation from several pinning points. Materials Science and Engineering: A. 2001;**309-310**:203-206. DOI: 10.1016/S0921-5093(00)01792-5

[27] Gremaud G. Dislocation-point defect interactions. Materials Science Forum. 2001;**366-368**:178-246. DOI: 10.4028/www.scientific.net/MSF.366-368.178

[28] Dotsenko VI. Stress relaxation in crystals. Physica Status Solidi B. 1979;**93**:11-43. DOI: 10.1002/pssb.2220930102

[29] Urusovskaya AA, Petchenko AM, Mozgovoi VI. The influence of strain rate on stress relaxation. Physica Status Solidi (A). 1991;**125**:155-160. DOI: 10.1002/pssa.2211250112

[30] Johnston WG, Gilman JJ. Dislocation velocities, dislocation densities, and plastic flow in lithium fluoride crystals. Journal of Applied Physics. 1959;**30**:129-144. DOI: 10.1063/1.1735121

[31] Granato AV, Lücke K. Theory of mechanical damping due to dislocations. Journal of Applied Physics. 1956;**27**:583-593. DOI: 10.1063/1.1722436

[32] Blaha F, Langenecker B. Dehnung von Zink-kristallen unter ultraschalleinwirkung. Naturwissenschaften. 1955;**42**:556. DOI: 10.1007/BF00623773

[33] Ohgaku T, Takeuchi N. The relation of the Blaha effect with internal friction for alkali halide crystals. Physica Status Solidi A: Applications and Material Science. 1988;**105**:153-159. DOI: 10.1002/pssa.2211050115

[34] Ohgaku T, Takeuchi N. Relation between plastic deformation and the Blaha effect for alkali halide crystals. Physica Status Solidi A: Applications and Material Science. 1989;**111**:165-172. DOI: 10.1002/pssa.2211110117

[35] Ohgaku T, Takeuchi N. Interaction between a dislocation and monovalent impurities in KCl single crystals. Physica Status Solidi A: Applications and Material Science. 1992;**134**:397-404. DOI: 10.1002/pssa.2211340210

[36] Ohgaku T, Teraji H. Investigation of interaction between a dislocation and a Br^- ion in NaCl:Br^- single crystals. Physica Status Solidi A: Applications and Material Science. 2001;**187**:407-413

[37] Ohgaku T, Hashimoto K. Strain rate sensitivity of flow stress under superimposition of ultrasonic oscillatory stress during plastic deformation of RbCl doped with Br^- or I^-. Materials Science and Engineering A. 2005;**400-401**:401-404. DOI: 10.1016/j.msea.2005.03.058

[38] Ohgaku T, Matsunaga T. Interaction between dislocation and divalent impurity in KBr single crystals. IOP Conference Series: Materials Science and Engineering. 2009;**3**:012021. DOI: 10.1088/1757-899X/3/1/012021

[39] Kohzuki Y. Study on the interaction between a dislocation and impurities in KCl:Sr^{2+} single crystals by the Blaha effect-part IV influence of heat treatment on dislocation density. Journal of Materials Science. 2009;**44**:379-384. DOI: 10.1007/s10853-008-3150-8

[40] Kohzuki Y. Bending angle of dislocation pinned by an obstacle and the Friedel relation. Philosophical Magazine. 2010;**90**:2273-2287. DOI: 10.1080/14786431003636089

[41] Ohgaku T, Migiuma S, Nagahira D. Interaction between dislocation and defects induced by X-irradiation in alkali halide crystals. Radiation Measurements. 2011;**46**:1385-1388. DOI: 10.1016/j.radmeas.2011.05.067

[42] Nevill GE, Brotzen FR. The effect of vibrations on the static yield strength of low-carbon steel. Journal of ASTM International. 1957;**57**:751-758

[43] Langenecker B. Effects of ultrasound on deformation characteristics of metals. IEEE Transactions on Sonics and Ultrasonics. 1966;**SU-13**:1-8. DOI: 10.1109/T-SU.1966.29367

[44] Izumi O, Oyama K, Suzuki Y. Effects of superimposed ultrasonic vibration on compressive deformation of metals. Materials transactions, JIM. 1966;**7**:162-167. DOI: 10.2320/matertrans1960.7.162

[45] Evans AE, Smith AW, Waterhouse WJ, Sansome DH. Review of the application of ultrasonic vibrations to deforming metals. Ultrasonics. 1975;**13**:162-170

[46] Jimma T, Kasuga Y, Iwaki N, Miyazawa O, Mori E, Ito K, et al. An application of ultrasonic vibration to the deep drawing process. Journal of Materials Processing Technology. 1998;**80-81**:406-412. DOI: 10.1016/S0924-0136(98)00195-2

[47] Susan M, Bujoreanu LG. The metal-tool contact friction at the ultrasonic vibration drawing of ball-bearing steel

wires. Revista de Metalurgia (Madrid). 1999;**35**:379-383. DOI: 10.3989/revmetalm.1999.v35.i6.646

[48] Murakawa M, Jin M. The utility of radially and ultrasonically vibrated dies in the wire drawing process. Journal of Materials Processing Technology. 2001;**113**:81-86. DOI: 10.1016/S0924-0136(01)00635-5

[49] Susan M, Bujoreanu LG, Găluşcă DG, Munteanu C, Mantu M. On the drawing in ultrasonic field of metallic wires with high mechanical resistance. Journal of Optoelectronics and Advanced Materials. 2005;**7**:637-645

[50] Lucas M, Gachagan A, Cardoni A. Research applications and opportunities in power ultrasonics. Proceedings of the Institution of Mechanical Engineers, Part C. 2009;**223**:2949-2965. DOI: 10.1243/09544062JMES1671

[51] Siddiq A, El Sayed T. Ultrasonic-assisted manufacturing processes: Variational model and numerical simulations. Ultrasonics. 2012;**52**:521-529. DOI: 10.1016/j.ultras.2011.11.004

[52] Makhdum F, Phadnis VA, Roy A, Silberschmidt VV. Effect of ultrasonically-assisted drilling on carbon-fibre-reinforced plastics. Journal of Sound and Vibration. 2014;**333**:5939-5952. DOI: 10.1016/j.jsv.2014.05.042

[53] Graff KF. Ultrasonic metal forming: Processing. In: Gallego-Juarez JA, Graff KF, editors. Power Ultrasonics: Applications of High-Intensity Ultrasound. Cambridge UK: Elsevier; 2015. pp. 377-438

[54] Cottrell AH, Bilby BA. Dislocation theory of yielding and strain ageing of iron. Proceedings of the Physical Society of London. 1949;**62**:49-62. DOI: 10.1088/0370-1298/62/1/308

[55] Pamplin BR, editor. Introdction to crystal growth methods. In: Crystal Growth. Pergamon Press: Oxford; 1975. pp. 1-11

[56] Sirdeshmukh DB, Sirdeshmukh L, Subhadra KG. In: Hull R, Osgood RM, Sakaki H Jr, Zunger A, editors. Alkali Halides: A Handbook of Physical Properties. Berlin Heidelberg: Springer-Verlag; 2001. p. 41

[57] Conrad H. Thermally activated deformation of metals. Journal of Metals. 1964;**16**:582-588. DOI: 10.1007/BF03378292

[58] Kohzuki Y, Ohgaku T. Activation energy for dislocation breakaway from various monovalent ions in NaCl single crystals. Philosophical Magazine. 2016;(96):3109-3119. DOI: 10.1080/14786435.2016.1227099